Cancer Management and Research

Dovepress

open access to scientific and medical research

Open Access Full Text Article

ORIGINAL RESEARCH

WAVE2 Enhanced Hepatic Stellate Cells Activity in Colorectal Liver Metastases

This article was published in the following Dove Press journal:
Cancer Management and Research

Fengbo Tan[1,2]
Dongren He[2]
Kuan Hu[1,2]
Dong Wang[2]
Sai Zhang[3]
Juanni Li[4]
Zhiming Wang[1,2]
Yiming Tao[1]

[1]Department of General Surgery Research, Xiangya Hospital, Central South University, Changsha, Hunan, People's Republic of China; [2]Department of General Surgery, Xiangya Hospital, Central South University, Changsha, Hunan, People's Republic of China; [3]Institute of Medical Sciences, Xiangya Hospital, Central South University, Changsha, Hunan, People's Republic of China; [4]Department of Pathology, Xiangya Hospital, Central South University, Changsha, Hunan, People's Republic of China

Background: Cancer cell migration, tumor angiogenesis, and activated hepatic stellate cells (a-HSCs) promote the development of colorectal liver metastases (CLM). Wiskott–Aldrich syndrome protein family verprolin-homologous protein 2 (WAVE2) has been associated with CLM, although the underlying molecular mechanisms remain unclear.

Methods: In the current study, we evaluated the relationship between WAVE2 and CLM in 103 CLM patients who underwent liver resection. Immunohistochemistry (IHC) staining was performed to determine the association between WAVE2 protein expression and hepatic micro-metastasis in human CLM tissues. WAVE2 knockout was performed in hepatic stellate cells (HSC) to explore the function and signaling pathways of WAVE2 in colorectal cancer progression.

Results: Significantly higher levels of WAVE2 were detected in portal-associated relative to sinusoid-associated micro-metastasis. A strong correlation was identified between WAVE2 levels and microvessel density (MVD) in hepatic metastasis. Similarly, expression of WAVE2 was closely associated with activation of HSCs. Mechanistically, WAVE2 regulated the progression of human CLM acts by regulating the growth factor β (TGF-β) and Hippo pathways via effector yes-associated protein (YAP1).

Conclusion: Overall, our results demonstrated that WAVE2 participates in CLM tumor microenvironment, and can be a potential latent therapeutic target for CLM.

Keywords: colorectal cancer, hepatic stellate cells, liver metastasis, WAVE2

Introduction

The liver is a common site for colorectal cancer (CRC) metastases, a disease that causes cancer-related deaths worldwide.[1] Numerous studies suggest that the ability of cancer cells to metastasize and proliferate in the liver depends on their surrounding microenvironment.[2] In fact, rapid growth of liver metastases requires angiogenesis[3] and is further dependent on the activated hepatic stellate cells (a-HSCs) that support tumor growth. Besides being associated with tumor cells, inflammatory cytokines, and tumor-derived factors,[4] HSCs have also been implicated in angiogenesis processes.[5] Although we currently understand that HSC regulates colorectal liver metastases (CLM),[6] the underlying mechanism remain elusive.

Angiogenesis, the central pathological process in solid cancer, was reportedly most active at the tumor invading edge, and has a close relationship with a-HSCs.[7] Previous studies have demonstrated that transforming growth factor β (TGF-β) and the Hippo pathway effector Yes-associated protein (YAP1) are the most significant pathways regulating a-HSCs.[8,9] Therefore, exploring the molecular changes across these pathways presents an opportunity for identifying novel targets for CLM

Correspondence: Yiming Tao
Department of General Surgery Research, Xiangya Hospital, Central South University, Changsha, Hunan, People's Republic of China
Tel +86-731-8432-7191
Fax +86-731-8975-3510
Email yimingtao@csu.edu.cn

submit your manuscript | www.dovepress.com
DovePress
http://doi.org/10.2147/CMAR.S259125

treatment. Wiskott–Aldrich syndrome protein family verprolin-homologous protein 2 (WAVE2), a crucial regulator of cell migration, has been shown to affect embryonic vascular development and play a role in angiogenesis.[10]

In vivo studies have shown that this factor regulates remodeling of actin cytoskeleton by activating the actin-related protein 2 and 3 (Arp2/3) complex, thereby inhibiting embryonic fibroblasts (MEFs) in mice. Furthermore, overexpression of WAVE2 has been linked to poor prognosis and high metastasis of hepatocellular carcinoma (HCC).[11,12] Other recent studies have shown that WAVE2 proteins mediate tumor progression in lung,[13] and breast[14] cancers as well as CLM.[15] However, the mechanism through which this factor accelerates the metastasis of CRC in the liver remains unknown. In this study, the contributions of WAVE2 and a-HSCs to CLM were explored.

Materials and Methods

Study Design

We performed a retrospective study to examine expression profiles of WAVE2 in CLM patients undergoing curative resection, and evaluated the role of this genetic factor in a-HSCs using in vivo and in vitro experiments.

Ethical Approval

Clinical studies were conducted in accordance with guidelines in the Helsinki Declaration. Informed consent was obtained from all patients prior to their enrolment in the study. All procedures complied with ethical guidelines and were approved by the ethics committee of XiangYa Hospital Central South University, Permit Number: 201,103,768.

Human CLM Specimens

Surgical tumor specimens were collected from 103 CLM patients at XiangYa Hospital, China. The clinical data of these patients have been collected for further research (Supplementary Table). None of these patients had undergone chemotherapy. Patients were divided into two groups, comprising those with sinusoid-associated micro-metastasis (SAM) and portal-associated micro-metastasis (PAM), according to Solaun et al.[16]

Establishment of Cell Cultures and Transfections

Human CRC cells, HT-29, were purchased from American Type Culture Collection (ATCC) (Manassas, VA, USA), and cultured in Dulbecco's modified Eagle's medium (DMEM) supplemented with 10% fetal bovine serum (FBS) and 100U/mL penicillin, and 100 mg/mL streptomycin. Packaging lentiviruses encoding non-targeting short hairpin RNAs (sh-NT) and WAVE2 shRNA (sh-WAVE2) were purchased from Santa Cruz Biotechnology (NM_001201404-Q9Y6W5 and NM_006990-605875; Cat# sc-36833-V), whereas si-YAP was acquired from Guangzhou RiboBio (Guangzhou, China). The cells were inoculated into the culture for viral transduction, subcultured into sterile DMEM, supplemented with 10% FBS for 2–3 days, then harvested for subsequent experiments.

Establishment of Primary HSC Cultures

Isolation of HSCs was performed as described by Dou et al.[17] Briefly, mice were anesthetized using ketamine (100 mg/kg) and xyaline (10 mg/kg), then a surgical incision made in the middle line of the belly, to expose the portal vein. Thereafter, a cell pellet was layered on a discontinuous density gradient and cultured in 35 mm Petri-dishes containing 10% fetal bovine serum. Purified q-HSC and in vitro a-HSC populations were immediately subjected to Immunofluorescence (IF).

Immunohistochemistry (IHC)

IHC staining was performed as described by Yang et al.[11] Summarily, deparaffinization and antigen retrieval were performed in EDTA buffer (1 mM, pH 8.0) by microwave, then 4 μm-thick formalin-fixed tissue sections were incubated overnight with primary antibody at 4°C. Slides were subsequently incubated with the secondary antibody, conjugated with streptavidin-biotin-peroxidase complex (LSAB2/HRP kit, DAKO, Denmark), then a color reaction developed using 3, 3-diaminobenzidine tetrahydrochloride (Sigma-Aldrich, St Louis, MO). Antibody dilution was carried out at a ratio of 1:500, for the WAVE2 polyclonal antibodies (Cat. #YT4898, ImmunoWay). IHC staining was analyzed and scored using the full-slide digitalization Panoramic Scan and the database-linked TMA Modul software (3DHISTECH, Budapest, Hungary). A blinded analysis of the result was independently performed, using the H-score method, by two experienced pathologists (Juanni Li and Lian Zeng). Staining analysis and quantification was also done by the 2 pathologists using H-scores according to the following equation: H-score = ("3+" % cells)*3 + ("2+" % cells)*2 + ("1+" % cells)*1 + (0% cells)*0, where "0" denotes no staining, whereas "1+, 2+, and +3" indicate weak, moderate, and strong staining, respectively.

The sections were stained with CD31 monoclonal antibody, then tumor microvessels, analyzed by calculating their average number, any brown-stained endothelial cell or endothelial cell cluster that was clearly separated from adjacent microvessels. Tumor cells and connective elements were counted as 1 microvessel, irrespective of presence of a vessel lumen. Microvascular density (MVD) scoring was performed as described by Tao et al.[18]

Western Blot (WB) Assay

Proteins were first extracted using the radio immunoprecipitation assay lysis buffer, containing phenylmethylsulfonyl fluoride, Na2VO3, NaF and protease inhibitors (Roche, Cat. # 11873580001). Protein (50 μg) was then denatured on 10–14% sodium dodecyl sulfate polyacrylamide gels (SDS-PAGE) and transferred onto a nitrocellulose membrane as previously described.[12] WAVE2 polyclonal antibodies (Cat. #YT4898, ImmunoWay), including alpha-smooth muscle actin (α-SMA) (abcame, Cat. # ab5831), phosphorylated mothers against decapentaplegic homolog 2 (p-SMAD2) (CST, Cat. # 3101), and transforming growth factor-beta receptor 2 (TβRII) polyclonal antibody (Santa Cruz Biotechnology, Cat. # sc-17791) were diluted at a ratio of 1:1000, whereas β-actin mouse monoclonal antibody (Sigma-Aldrich, Cat. # A1978) was diluted at 1:5000. Images (WB) were subjected to Image J software (NIH) for analysis of signal intensity.

Quantitative Real Time Polymerase Chain Reaction (qRT-PCR)

Total ribonucleic acid (RNA) was isolated using the RNeasy extraction kit (Invitrogen, Carlsbad, CA) according to the manufacturer's instructions, then reverse-transcribed to complementary deoxyribonucleic acid (cDNA) using the iScript™ cDNA Synthesis Kit (QIAGEN). qRT-PCR was then carried out on an ABI Prism 7500 Sequence Detection System (Applied Biosystems), using SYBR Premix Ex Taq II (TakaRa) as described in the kit.[19] Glyceraldehyde-3-phosphate dehydrogenase (GAPDH) was also included, as an internal amplification control, with fold changes of target mRNA expression analyzed relative to GAPDH. All experiments were performed in triplicates.

Fluorescence Microscopy Assay

Immunofluorescence (IF) staining was performed according to a protocol by Tan et al.[20] Briefly, treated cells were washed with cold phosphate-buffered saline (PBS, pH 7.4), fixed with 3% paraformaldehyde, followed by infiltration with 0.1% Triton X-100 and a 30-minute incubation with 5% BSA in PBS containing 0.05% Tween-20 (PBS-t). Thereafter, IF staining was performed in triplicate.

Generation of Media Conditioned by Tumor-Activated HSCs

HT-29-conditioned medium (HT-29-CM) was obtained by diluting the supernatant from sub-confluent HT-29 cell cultures, preserved for 24 hours in serum-free DMEM media, with fresh media (1:1). The HSCs isolated 48 hours before, were maintained for 24 hours in basal serum-free media to obtain untreated HSC-CM, and in H-T29-CM for tumor-activated HSC-CM. All experiments were performed in triplicate.

In vivo Orthotopic Implantation Assay

Ethical approval was approved by the Ethics Committee of XiangYa Hospital Central South University (Changsha, China), Permit Number: N02019030913. All animal care and procedures were performed according to the guiding opinions on treating experimental animals well formulated the ministry of science and technology of China. Orthotopic implantation was performed as previously described.[21] Briefly, HT29-mixed HSC cells (7×10^6), transduced with shNC or shWAVE2, were subcutaneously injected into the dorsal surfaces of female athymic BALB/c nude mice (6 mice/group). Once the xenografts were established, tumors were excised and minced into 3 (1 mm) pieces, then two pieces orthotopically implanted into the liver of another athymic nude mouse. The animals were anesthetized by isoflurane inhalation prior to operation. Tumor-bearing mice were sacrificed, 4 weeks after tumor cell inoculation, then histopathology section for each orthotropic transplantation tumor analyzed for immunoreactivity against α-SMA and CD31.

Bioinformatics Analysis

A correlation between expression profiles of WAVE2 mRNAs and HSCs levels in colon adenocarcinoma (COAD) and rectum adenocarcinoma (READ) was done using the online database, Gene Expression Profiling Interactive Analysis (GEPIA) (http://gepia.cancer-pku.cn/).[22]

Statistical Analyses

Data were analyzed using GraphPad Prism 7 software (GraphPad Software, Inc., La Jolla, CA), then expressed as means ± standard deviation (SD) of the means. Comparisons between groups were done using a two-tailed Student's *t*-test. A Pearson's correlation was also performed to analyze the relationship between WAVE2 expression and MVD. Values followed by $P < 0.05$ were considered statistically significant.

Results

Relationship Between WAVE2 Protein Expression and Hepatic Micro-Metastasis

Analysis of all metastases revealed that 64% were Sinusoid-associated micro-metastasis, containing non-encapsulated reticularly-arranged myofibroblasts, whereas 36% of them were PAM, and comprised incompletely encapsulated fibrous tract–arranged myofibroblasts (Figure 1A). The two hepatic micro-metastasis variants, SAM and PAM, were identified by Cytokeratin 20 (CK20) IHC staining examination (Figure 1B), a well-established CLM marker.[23] Effect of microvascular density (MVD) on prognosis in CLM,[24] calculated using CD31 (Figure 1C), revealed higher levels of WAVE2 expression in PAM than SAM (Figure 1D and E). In addition, Pearson correlation analysis revealed a positive correlation between WAVE2 and MVD in hepatic metastasis ($r = 0.697$; $P < 0.001$) (Figure 1F). Overall, these findings suggest that WAVE2 acts as an oncogene that promotes CLM.

WAVE2 Knockdown Impairs Paracrine Effects of a-HSCs on Tumor Progression

Since CLM-isolated HSCs in culture cells express WAVE2, we transduced HSCs with shWAVE2 (Figure 2A). Previous studies have shown that Actin cytoskeleton remodeling is a perquisite for TGF-β1-mediated myofibroblastic activation in HSCs.[25] Consequently, we investigated whether WAVE2 could regulate myofibroblastic activation of HSCs via the TGF-β1 signaling pathway. Results showed that in the control cells, 24-hour stimulation of TGF-β1 induced development of α-SMA positive stress fibers in more than 60% of cells, indicating that successful myofibroblastic activation in the HSCs. Conversely, knockdown of WAVE2 inhibited TGF-β1 activation of HSCs, as evidenced by α-SMA IF-based quantification (Figure 2B). Western blots revealed significantly lower activation of both α-SMA and p-SMAD2 in shWAVE2-transfected HSC, relative to control cells (Figure 2C).

WAVE2 Mediates Activation of HSCs via the YAP1 Signaling Pathway

A positive correlation was found between WAVE2 mRNA expression and activation of HSCs genes in colon adenocarcinoma (COAD) as well as rectum adenocarcinoma (READ) (Supplementary Figure S1). WAVE2 was also positively correlated with expression of p300,[26] hypoxia-inducible factor (HIF-1α)[27] and Yes-associated protein 1 (YAP1).[9] We also investigated the effect of YAP1 signaling cascade on WAVE2 inactivation of HSC processes, since these factors has been shown to play a critical role in HSC activation.[28] Western blots showed that Si-YAP1 knockdown significantly decreased expression levels of WAVE2, α-SMA and p-SMAD2 (Figure 3A), in line with Pefani et al[29] who reported that TGF-β1 targets the Hippo pathway to facilitate YAP1/SMAD2 signaling. Moreover, WAVE2 expression correlated with reduced YAP1 levels, and resulted in reduced nuclear translocation efficiency as well as increased cytoplasmic retention of SMAD2 association (Figure 3B).

WAVE2 Promotes CLM in vivo Through a Paracrine Mechanism

Mice in the HT29+HSC-shWAVE2 group exhibited lower tumor weights compared to those in the HT29+HSC-WAVE2 group, at 1.552 ± 0.11 and 1.014 ± 0.17g, respectively, although these were not significantly different ($P = 0.029$) (Figure 4A). Moreover, IF staining of α-SMA revealed higher levels of a-HSCs in the control than the HT29+HSC-shWAVE2 group (Figure 4B), whereas Immunohistochemistry targeting CD31 showed that tumor cells in HT29+HSC-shNC had significantly higher ($P<0.001$) MVD than those in the HT29+HSC-shWAVE2 group, at 37.35 ± 3.66 and 18.72 ± 1.04, respectively (Figure 4C). This was rational because myofibroblast infiltration precedes angiogenesis in hepatic metastasis.[30] These findings suggest that activation of the TGF-β1/YAP1 signaling pathway could transduce the effects of WAVE2 on HSCs during CLM pathogenesis in mice (Figure 5).

Discussion

Previous studies have reported high expression of WAVE2 in CRC tissues, as well as its association with disease

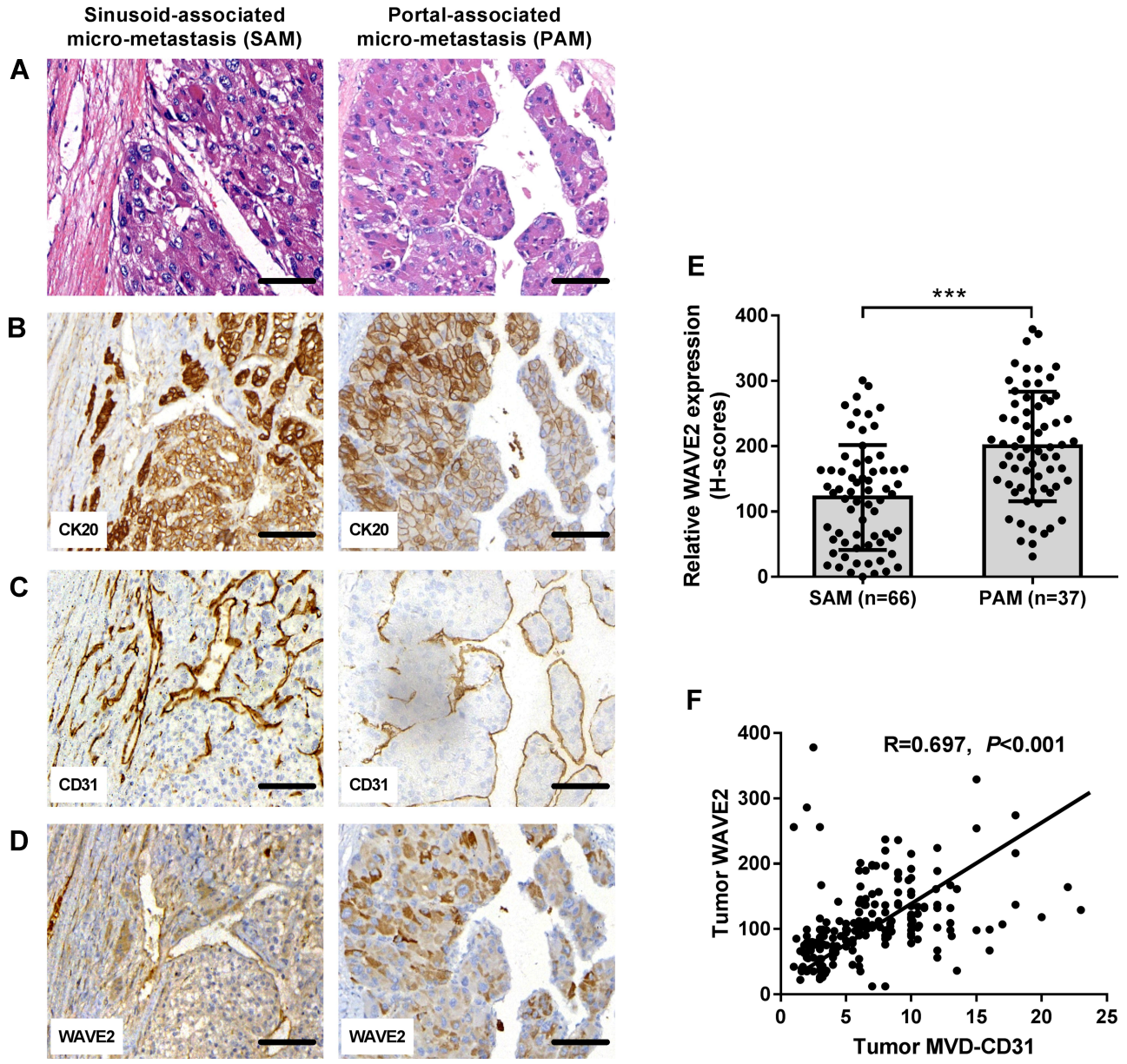

Figure 1 Association between WAVE2 protein expression and hepatic micro-metastasis in human CLM. (**A**) Profiles of sinusoid-associated micro-metastasis (SAM) and portal-associated micro-metastasis (PAM) following H&E staining. (**B**) Detection of CLM in hepatic tissue sections via immunohistochemical staining with CK20. (**C**) Profiles of CD31-labeled MVD in CLM. (**D**) Immunohistochemical staining of WAVE2 protein expression in SAM and PAM. Scale bar=50 μm. (**E**) PAM lesions exhibit higher WAVE2 protein levels than SAM lesions. Quantification of WAVE2 expression by H-score is also shown. *** $P<0.001$. (**F**) The relationship between WAVE2 and MVD in CLM. *** $P<0.001$.

progression and liver metastasis.[15] However, expression of this factor in metastatic colorectal cancer tissues remains unclear. In the present study, IHC staining results from the colorectal CLM cohort revealed an association of WAVE2 expression with liver metastasis and microvessel density. Moreover, WAVE2 was highly expressed in the PAM group which through the portal vein to form metastatic carcinoma. In addition, expression of WAVE2 in HSC was correlated with activation of the TGF-β1 and YAP1 signaling pathways. Overall, these findings strongly suggested that WAVE2 plays a critical role in CLM progression.

Previous study showed that HSCs are a component of the pro-metastatic liver microenvironment. Stimulation of these cells triggers their transdifferentiation into highly proliferative and motile myofibroblasts. Desmoplastic reaction between tumors and HSCs may function as a sensor, to further enhance metastatic growth in the

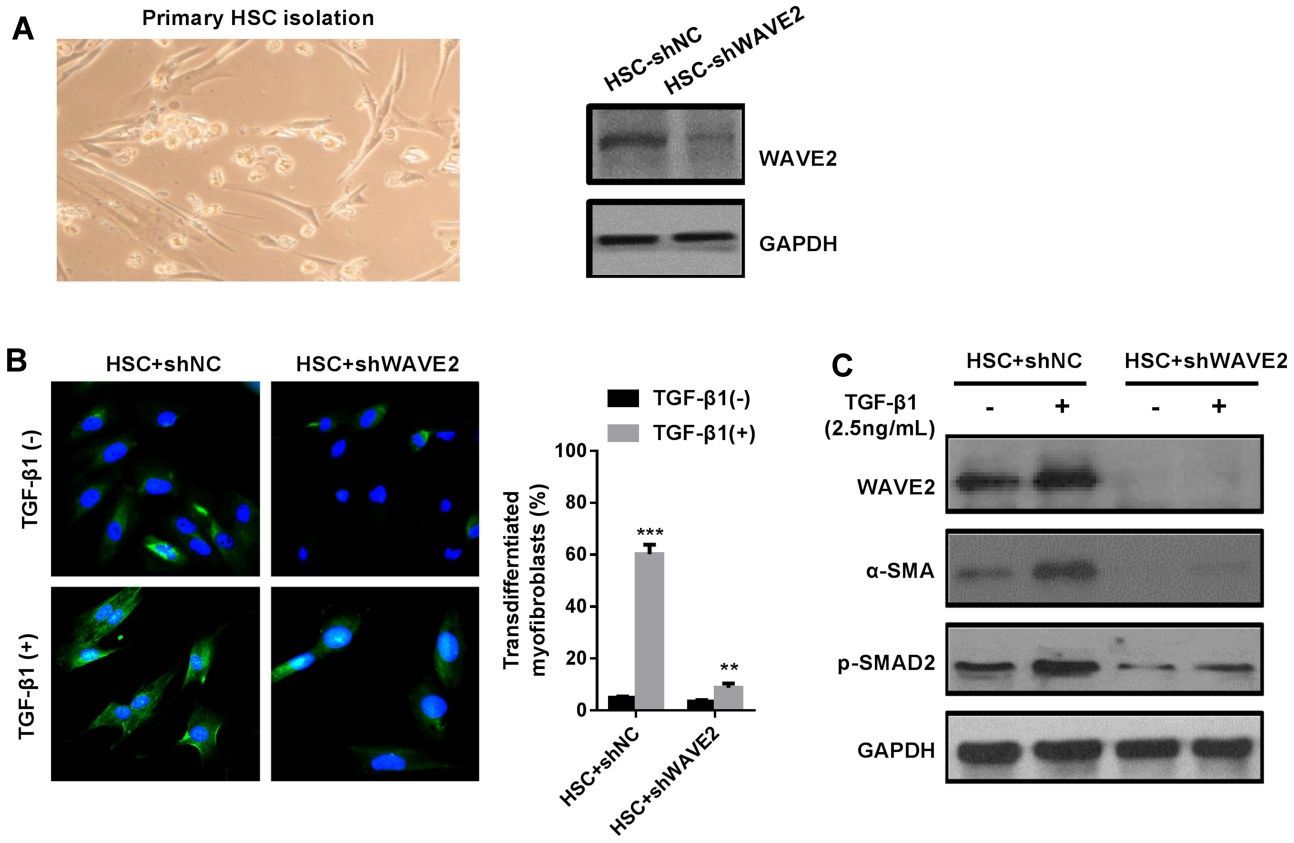

Figure 2 WAVE2 knockdown inhibits activation of HSCs into tumor-associated myofibroblasts. (**A**) Downregulation of WAVE2 expression via shWAVE2 lentiviral knockdown in human HSCs cells. Western blots showing efficiently-knocked down WAVE2. (**B**) HSCs transduced with shNC or shWAVE2 lentiviruses, treated with TGF-β1 (2.5 ng/mL) and subjected to IF for α-SMA (green). WAVE2 knockdown consistently suppressed TGF-β1 activation of HSCs into myofibroblasts. Bar=50 mm. ***P*<0.01, ****P*<0.001; n=5 randomly picked microscopic fields. (**C**) Control and WAVE2 knockdown HSCs, serum-starved and treated with TGF-β1 after 24 hours. Cell lysates were subjected to Western blot analysis for detection of HSC activation markers, α-SMA and p-SMAD2.

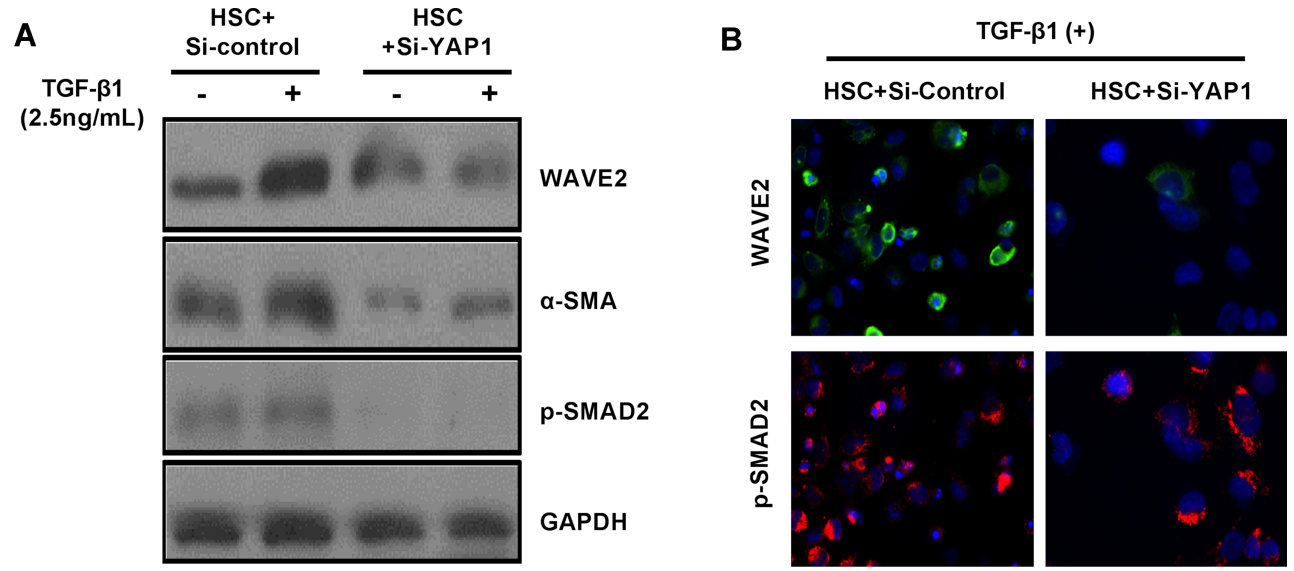

Figure 3 WAVE2/YAP1 signaling is a critical driver of activation of HSC processes. (**A**) Western blots of HSC activation showing lower levels of WAVE2, α-SMA and p-SMAD2 in Si-YAP1-transfected HSC cells relative to controls. (**B**) IF analysis for WAVE2 (green) and p-SMAD2 (red).

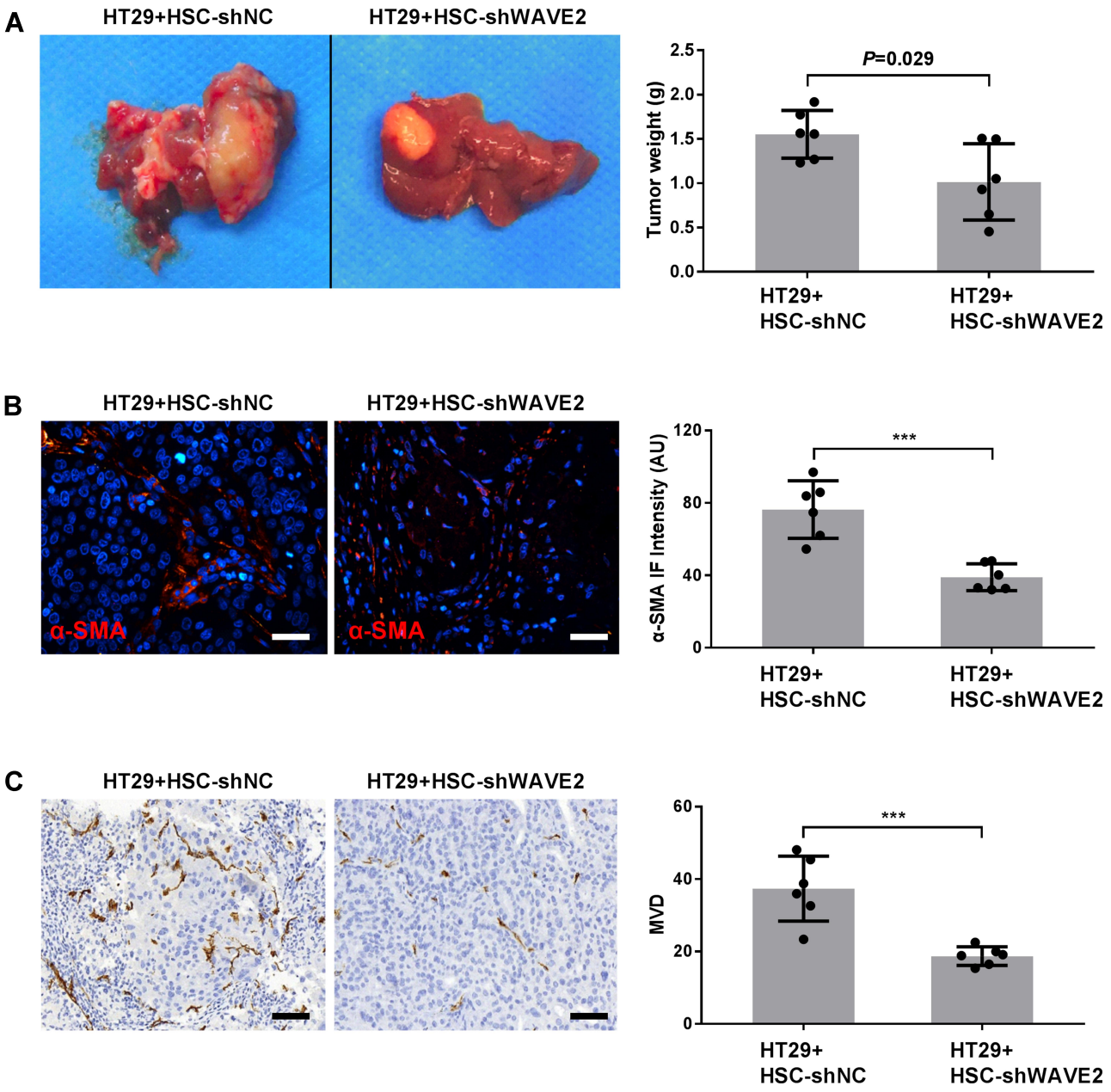

Figure 4 WAVE2 knockdown reduces stimulatory effects of HSCs on tumor prognosis in mice. (**A**) HT29 cells (0.5×10^6) mixed with 0.5×10^6 a-HSCs expressing either sh-NC or sh-WAVE2 were implanted into nude mice by orthotropic transplantation. Images of dissected tumors from mice (left) and the tumor size between the HT29+HSC-shNC and HT29+HSC-shWAVE2 groups (right) were compared. Each bar represents mean ± SD of six mice per group. (**B**) IF staining for α-SMA detection showing that WAVE2 knockdown HSCs impairs HT29 tumor growth in mice. *** $P<0.001$ (**C**) IHC staining of CD31 in xenograft. *** $P<0.001$.

liver,[31] which has been confirmed to be a highly vascularized organ that frequently hosts metastases in patients with colorectal adenocarcinomas. Therefore, dysregulated WAVE2 expression might be an indicator for its potential as a biomarker and therapeutic target in CLM.

Notably, our animal models revealed an association between WAVE2 with HSC activation and MVD formation. This is consistent with the findings of Brodt et al,[2] who demonstrated that a-HSCs are not a binary process but occurs through distinct cellular states in the microenvironment. HSC activation and recruitment, into metastatic nodules, is essential for tumor angiogenesis and may depend on various mechanisms, such as tumor cell-derived soluble factors, hypoxia, proinflammatory cytokines and release of reactive oxygen.[30] In the current study, we focused on WAVE2's intracellular signaling pathway, to understand its synergist effects.

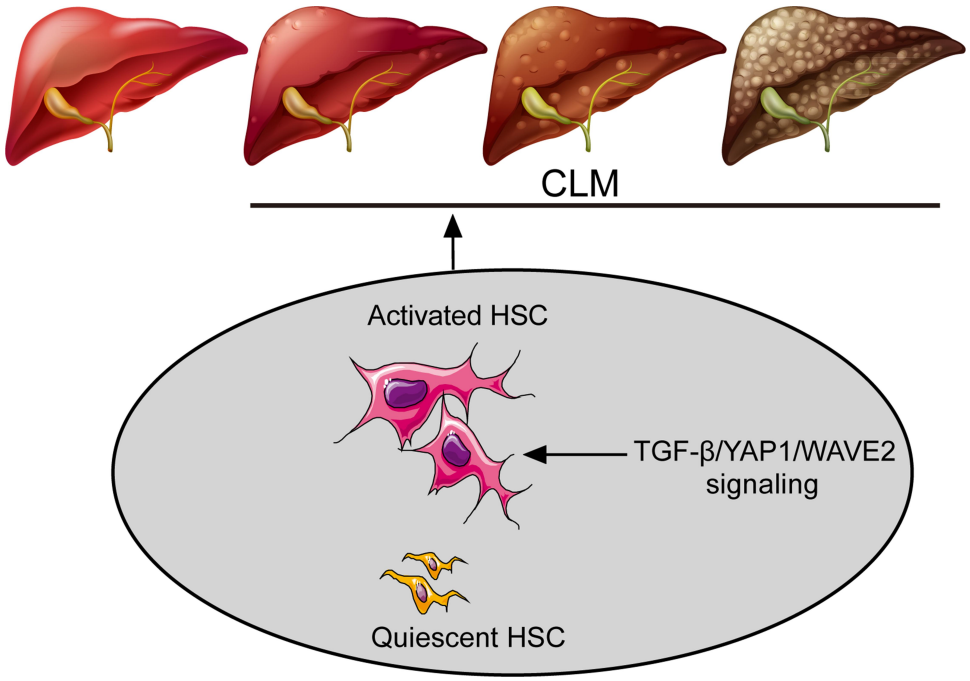

Figure 5 Schematic diagram showing the effect of WAVE2 on HSC processes and paracrine signaling in the tumor microenvironment. WAVE2 was associated with regulatory functions of the TGF-β1/YAP1 signaling in CLM pathogenesis.

Increasing evidence has shown that tumor microenvironment and immune infiltration play a critical role in tumor development and progression. For example, Park et al.[32] found that TGF-β1 was involved in cancer immune microenvironment and promoted metastasis of liver tumors. In the present study, TGF-β1 mediated WAVE2 upregulation on HSC activation, and also promoted a-HSCs metastasis both in vitro and in vivo. Previous studies have shown that TGF-β and YAP1 are essential for HSC activation.[33] In addition, WAVE2 in the tumor microenvironment has been found to suppress TβRII and TGF-β dependent myofibroblastic differentiation, thus constraining tumor growth.[34] These observations suggest the existence of a key signaling pathway involving WAVE2 and YAP1 driving liver metastasis. Additionally, HSCs were recently found to induce T cell hyporesponsiveness and regulate T cell expansion, a process that involves CLM,[35] whereas WAVE2 was shown to act as an Actin-regulatory protein. Furthermore, the mechanism through which these proteins control T cell function has also been proposed.[36] Future studies are expected to evaluate efficacy of administering a vascular endothelial growth factor (VEGF) inhibitor with chemotherapeutic agents containing WAVE2 for prevention and treatment of liver metastasis. Since previous studies on the effect of WAVE2 in tumor immune microenvironment are limited to CLM, our findings provide a baseline for future identification of new biomarkers and development of novel therapeutic approaches for CLM.

Conclusions

In summary, our results demonstrate that WAVE2 is a key indicator of CLM, thus a potential target for development of novel treatments of CLM. This study further provides important insights into the role of WAVE2 in other types of cancers. Our findings may be limited, owing to the fact that this was a single center study. Consequently, large-scale prospective studies are needed to validate these results.

Data Sharing Statement

Data are available from the corresponding author upon reasonable request.

Acknowledgment

Thanks to freescience (www.home-for-researchers.com) for providing language polish in this manuscript.

Disclosure

The authors declare that they have no conflicts of interest for this work.

References

1. Dekker E, Tanis PJ, Vleugels JLA, Kasi PM, Wallace MB. Colorectal cancer. *Lancet*. 2019;394(10207):1467–1480. doi:10.1016/S0140-6736(19)32319-0

2. Brodt P. Role of the microenvironment in liver metastasis: from pre- to prometastatic niches. *Clin Cancer Res*. 2016;22(24):5971–5982. doi:10.1158/1078-0432.CCR-16-0460
3. Hanahan D, Weinberg RA. Hallmarks of cancer: the next generation. *Cell*. 2011;144(5):646–674. doi:10.1016/j.cell.2011.02.013
4. Olaso E, Santisteban A, Bidaurrazaga J, Gressner AM, Rosenbaum J, Vidal-Vanaclocha F. Tumor-dependent activation of rodent hepatic stellate cells during experimental melanoma metastasis. *Hepatology*. 1997;26(3):634–642. doi:10.1002/hep.510260315
5. Taura K, De Minicis S, Seki E, et al. Hepatic stellate cells secrete angiopoietin 1 that induces angiogenesis in liver fibrosis. *Gastroenterology*. 2008;135(5):1729–1738. doi:10.1053/j.gastro.2008.07.065
6. Kurisu S, Suetsugu S, Yamazaki D, Yamaguchi H, Takenawa T. Rac-WAVE2 signaling is involved in the invasive and metastatic phenotypes of murine melanoma cells. *Oncogene*. 2005;24(8):1309–1319. doi:10.1038/sj.onc.1208177
7. Zhang F, Lu S, He J, et al. Ligand activation of PPARγ by ligustrazine suppresses pericyte functions of hepatic stellate cells via SMRT-mediated transrepression of HIF-1α. *Theranostics*. 2018;8(3):610–626. doi:10.7150/thno.22237
8. Jin X, Aimaiti Y, Chen Z, Wang W, Li D. Hepatic stellate cells promote angiogenesis via the TGF-β1-jagged1/VEGFA axis. *Exp Cell Res*. 2018;373(1–2):34–43. doi:10.1016/j.yexcr.2018.07.045
9. Du K, Hyun J, Premont RT, et al. Hedgehog-YAP signaling pathway regulates glutaminolysis to control activation of hepatic stellate cells. *Gastroenterology*. 2018;154(5):1465–1479.e1413. doi:10.1053/j.gastro.2017.12.022
10. Yamazaki D, Suetsugu S, Miki H, et al. WAVE2 is required for directed cell migration and cardiovascular development. *Nature*. 2003;424(6947):452–456. doi:10.1038/nature01770
11. Yang L-Y, Tao Y-M, Ou D-P, Wang W, Chang Z-G WF. Increased expression of Wiskott-Aldrich syndrome protein family verprolin-homologous protein 2 correlated with poor prognosis of hepatocellular carcinoma. *Clin Cancer Res*. 2006;12(19):5673–5679. doi:10.1158/1078-0432.CCR-06-0022
12. Tao Y, Hu K, Tan F, et al. SH3-domain binding protein 1 in the tumor microenvironment promotes hepatocellular carcinoma metastasis through WAVE2 pathway. *Oncotarget*. 2016;7(14):18356–18370. doi:10.18632/oncotarget.7786
13. Semba S, Iwaya K, Matsubayashi J, et al. Coexpression of actin-related protein 2 and Wiskott-Aldrich syndrome family verproline-homologous protein 2 in adenocarcinoma of the lung. *Clin Cancer Res*. 2006;12(8):2449–2454. doi:10.1158/1078-0432.CCR-05-2566
14. Iwaya K, Norio K, Mukai K. Coexpression of Arp2 and WAVE2 predicts poor outcome in invasive breast carcinoma. *Mod Pathol*. 2007;20(3):339–343. doi:10.1038/modpathol.3800741
15. Iwaya K, Oikawa K, Semba S, et al. Correlation between liver metastasis of the colocalization of actin-related protein 2 and 3 complex and WAVE2 in colorectal carcinoma. *Cancer Sci*. 2007;98(7):992–999. doi:10.1111/j.1349-7006.2007.00488.x
16. Solaun MS, Mendoza L, De Luca M, et al. Endostatin inhibits murine colon carcinoma sinusoidal-type metastases by preferential targeting of hepatic sinusoidal endothelium. *Hepatology*. 2002;35(5):1104–1116. doi:10.1053/jhep.2002.32528
17. Dou C, Liu Z, Tu K, et al. P300 acetyltransferase mediates stiffness-induced activation of hepatic stellate cells into tumor-promoting myofibroblasts. *Gastroenterology*. 2018;154(8):2209–2221.e14. doi:10.1053/j.gastro.2018.02.015
18. Tao YM, Huang JL, Zeng S, et al. BTB/POZ domain-containing protein 7: epithelial-mesenchymal transition promoter and prognostic biomarker of hepatocellular carcinoma. *Hepatology*. 2013;57(6):2326–2337. doi:10.1002/hep.26268
19. Tan F, Huang Y, Pei Q, Liu H, Pei H, Zhu H. Matrix stiffness mediates stemness characteristics via activating the yes-associated protein in colorectal cancer cells. *J Cell Biochem*. 2018.
20. Tan F, Zhu H, Tao Y, et al. Neuron navigator 2 overexpression indicates poor prognosis of colorectal cancer and promotes invasion through the SSH1L/cofilin-1 pathway. *J Exp Clin Cancer Res*. 2015;34(1):117. doi:10.1186/s13046-015-0237-3
21. Agarwal E, Robb CM, Smith LM, et al. Role of Akt2 in regulation of metastasis suppressor 1 expression and colorectal cancer metastasis. *Oncogene*. 2017;36(22):3104–3118. doi:10.1038/onc.2016.460
22. Tang Z, Li C, Kang B, Gao G, Li C, Zhang Z. GEPIA: a web server for cancer and normal gene expression profiling and interactive analyses. *Nucleic Acids Res*. 2017;45(W1):W98–W102. doi:10.1093/nar/gkx247
23. Rullier A, Le Bail B, Fawaz R, Blanc JF, Saric J, Bioulac-Sage P. Cytokeratin 7 and 20 expression in cholangiocarcinomas varies along the biliary tract but still differs from that in colorectal carcinoma metastasis. *Am J Surg Pathol*. 2000;24(6):870–876. doi:10.1097/00000478-200006000-00014
24. Rajaganeshan R, Prasad R, Guillou PJ, et al. The influence of invasive growth pattern and microvessel density on prognosis in colorectal cancer and colorectal liver metastases. *Br J Cancer*. 2007;96(7):1112–1117. doi:10.1038/sj.bjc.6603677
25. Wang XM, Yu DMT, McCaughan GW, Gorrell MD. Fibroblast activation protein increases apoptosis, cell adhesion, and migration by the LX-2 human stellate cell line. *Hepatology*. 2005;42(4):935–945.
26. Wang Y-C, Wu Y-S, Hung C-Y, et al. USP24 induces IL-6 in tumor-associated microenvironment by stabilizing p300 and β-TrCP and promotes cancer malignancy. *Nat Commun*. 2018;9(1):3996. doi:10.1038/s41467-018-06178-1
27. Orimo A, Tomioka Y, Shimizu Y, et al. Cancer-associated myofibroblasts possess various factors to promote endometrial tumor progression. *Clin Cancer Res*. 2001;7(10):3097–3105.
28. Mannaerts I, Leite SB, Verhulst S, et al. The Hippo pathway effector YAP controls mouse hepatic stellate cell activation. *J Hepatol*. 2015;63(3):679–688. doi:10.1016/j.jhep.2015.04.011
29. Pefani D-E, Pankova D, Abraham AG, et al. TGF-β targets the hippo pathway scaffold RASSF1A to facilitate YAP/SMAD2 nuclear translocation. *Mol Cell*. 2016;63(1):156–166. doi:10.1016/j.molcel.2016.05.012
30. Olaso E, Salado C, Egilegor E, et al. Proangiogenic role of tumor-activated hepatic stellate cells in experimental melanoma metastasis. *Hepatology*. 2003;37(3):674–685. doi:10.1053/jhep.2003.50068
31. Kang N, Gores GJ, Shah VH. Hepatic stellate cells: partners in crime for liver metastases? *Hepatology*. 2011;54(2):707–713. doi:10.1002/hep.24384
32. Park BV, Freeman ZT, Ghasemzadeh A, et al. TGFβ1-mediated SMAD3 enhances PD-1 expression on antigen-specific T cells in cancer. *Cancer Discov*. 2016;6(12):1366–1381. doi:10.1158/2159-8290.CD-15-1347
33. Perumal N, Perumal M, Halagowder D, Sivasithamparam N. Morin attenuates diethylnitrosamine-induced rat liver fibrosis and hepatic stellate cell activation by co-ordinated regulation of hippo/yap and TGF-β1/smad signaling. *Biochimie*. 2017;140:10–19. doi:10.1016/j.biochi.2017.05.017
34. Liu C, Billadeau DD, Abdelhakim H, et al. IQGAP1 suppresses TβRII-mediated myofibroblastic activation and metastatic growth in liver. *J Clin Invest*. 2013;123(3):1138–1156. doi:10.1172/JCI63836
35. Huang W-H, Zhou M-W, Zhu Y-F, et al. The role of hepatic stellate cells in promoting liver metastasis of colorectal carcinoma. *Onco Targets Ther*. 2019;12:7573–7580. doi:10.2147/OTT.S214409
36. Burkhardt JK, Carrizosa E, Shaffer MH. The actin cytoskeleton in T cell activation. *Annu Rev Immunol*. 2008;26(1):233–259. doi:10.1146/annurev.immunol.26.021607.090347